

Energy eigenstates of position-dependent mass particles in a spherical quantum dot

R. M. Lima* and H. R. Christiansen**

*CBPF – Centro Brasileiro de Pesquisas Físicas, CEP 22290-180, Rio de Janeiro, Brazil

**IFCE – Instituto Federal de Educação, Ciência e Tecnologia do Ceará, Maranguape, CEP 61940-750, Ceará, Brazil

corresponding author: hugo.christiansen@ifce.edu.br

Abstract

We obtain the exact energy spectrum of nonuniform mass particles for a collection of Hamiltonians in a three-dimensional approach to a quantum dot. By considering a set of generalized Schrödinger equations with different orderings between the particle's momentum and mass, the energy bound-states are calculated analytically for hard boundary conditions. The present results are of interest in atomic physics and quantum dot theory.

Keywords: quantum mechanics; position-dependent mass; exact solutions; quantum dots; atomic physics.

1 Introduction

Models for particles with nontrivial mass distributions have many uses, particularly for explaining electronic and optical properties of semiconductor devices such as nanowires, quantum dots and double heterostructures of diverse geometries [1–5]. Quantum dots have properties intermediate between bulk semiconductors and discrete atoms or molecules with similar spectral features. Semiconductor nanostructures, and solid-state quantum systems in general, can be studied by means of effective position-dependent mass (PDM) carriers stuck in order to simulate complex crystalline atomic effects. This theoretical approach has a long history [6–12].

The study of PDM differential equations has been steadily growing along the years, especially in one-dimensional models [13–19]. In more than one-dimension the literature is less abundant, *e.g.* [20–22].

The PDM problem is basically the fact that the ordinary Schrödinger differential equation becomes one dramatically more complex. Once we consider that the particle mass varies with position $M \rightarrow M(\mathbf{r})$ the differential equation suffers three main consequences. The ordinary energy eigenvalue E appears multiplied by a space function, the differential equation acquires new derivative terms and, on top of this, the kinetic energy operator is no longer unique so we may have an ambiguous quantum evolution and spectrum. Since the linear momentum $\hat{p} \equiv -i\hbar\nabla$ does not commute with the position operator (so neither with the particle mass), several Hamiltonians are possibly defined; this gives rise to the so-called ordering ambiguity (see, *e.g.*, [23, 24]). It is well known that the Schrödinger equation with external potentials has not met many cases with exact analytical solution. Thus, what was already a difficult task becomes much more complex when one considers a variable mass.

In order to handle such Hamiltonians altogether, we adopt a two-parameter hermitian operator [23]. In three dimensions, it reads

$$\hat{H}_{a,b}(\mathbf{r}) = -\frac{\hbar^2}{4} \left(M^a \hat{\nabla} M^{-1-a-b} \hat{\nabla} M^b + M^b \hat{\nabla} M^{-1-a-b} \hat{\nabla} M^a \right) + V(\mathbf{r}).$$

The parameters $a, b \in \mathbb{R}$ are to represent all the possible orderings and $V(\mathbf{r})$ is as usual an external potential. We will treat simultaneously the orderings of BDD (BenDaniel & Duke) [9] ($a = b = 0$), GW (Gora & Williams) [10] ($a = -1, b = 0$), ZK (Zhu & Kroemer) [11] ($a = b = -1/2$), LK (Li & Kuhn) [25] ($a = 0, b = -1/2$) and MM (Mustafa & Mazharimousavi) [24] ($a = b = -1/4$).

In three dimensions, the kinetic sector of the ordering family of Hamiltonians is

$$\hat{K}_{a,b}(\mathbf{r}) = \frac{1}{2M} \hat{\mathbf{p}}^2 - \frac{1}{2M} \left(\frac{1}{M} \hat{\mathbf{p}} M \right) \cdot \hat{\mathbf{p}} + \frac{1}{2M} \left[\frac{a+b}{2} \hat{\mathbf{p}} \left(\frac{1}{M} \hat{\mathbf{p}} M \right) - \left(ab + \frac{a+b}{2} \right) \left(\frac{1}{M} \hat{\mathbf{p}} M \right)^2 \right],$$

with $M \equiv M(\mathbf{r})$. The wave function $\Psi(\mathbf{r})$ thus obeys the following differential equation

$$-\nabla^2 \Psi(\mathbf{r}) + \frac{\nabla M}{M} \cdot \nabla \Psi(\mathbf{r}) + \frac{2M}{\hbar^2} (V(\mathbf{r}) + U_{a,b}(\mathbf{r})) \Psi(\mathbf{r}) = \frac{2M}{\hbar^2} E \Psi(\mathbf{r}), \quad (1)$$

where $U_{a,b}(\mathbf{r})$ contains all the ordering information in terms of a, b

$$U_{a,b}(\mathbf{r}) = -\frac{\hbar^2}{2M} \left[\frac{a+b}{2} \nabla \cdot \left(\frac{\nabla M}{M} \right) - \left(ab + \frac{a+b}{2} \right) \left(\frac{\nabla M}{M} \right)^2 \right]. \quad (2)$$

This potential $U_{a,b}(\mathbf{r})$ emerges independently of the presence of an external potential $V(\mathbf{r})$; it is just a direct consequence of considering a position-dependent mass.

By means of a scale transformation $\mathbf{r} \rightarrow \epsilon \mathbf{r}$, where $\epsilon > 0$ carries space units which make \mathbf{r} dimensionless, we introduce $\psi(\mathbf{r})$ and $m(\mathbf{r}) \equiv m$ such that $\Psi(\mathbf{r}) \rightarrow \epsilon^{-D/2} \psi(\mathbf{r})$ and $M(\mathbf{r}) \rightarrow m_0 m$, where D is the number of spatial dimensions and $m_0 > 0$ has mass units. Note the factor $\epsilon^{-D/2}$ guaranties the normalization condition invariant, *i.e.*, $1 = \int_{\mathbb{R}^D} |\Psi(\mathbf{r})|^2 d^D \mathbf{r} = \int_{\mathbb{R}^D} |\psi(\mathbf{r})|^2 d^D \mathbf{r}$. We also define the dimensionless energy functions $\tilde{E} \equiv \frac{2\epsilon^2 m_0}{\hbar^2} E$, $\tilde{V}(\mathbf{r}) \equiv \frac{2\epsilon^2 m_0}{\hbar^2} V(\epsilon \mathbf{r})$ and $\tilde{U}_{a,b}(\mathbf{r}) \equiv \frac{2\epsilon^2 m_0}{\hbar^2} U_{a,b}(\epsilon \mathbf{r})$. With this, the generalized Schrödinger equation above can be written in a simpler dimensionless form

$$-\frac{1}{m} \nabla^2 \psi(\mathbf{r}) + \frac{1}{m} \frac{\nabla m}{m} \cdot \nabla \psi(\mathbf{r}) + \left\{ -\frac{1}{m} \left[\frac{a+b}{2} \nabla \cdot \left(\frac{\nabla m}{m} \right) - \left(ab + \frac{a+b}{2} \right) \left(\frac{\nabla m}{m} \right)^2 \right] + \tilde{V}(\mathbf{r}) \right\} \psi(\mathbf{r}) = \tilde{E} \psi(\mathbf{r}). \quad (3)$$

We will solve this equation in the next sections.

2 Analytical solution

Since we aim to consider a spherical quantum dot, we proceed to separate the differential equation (3) using spherical coordinates (r, θ, ϕ) such that $x = r \cos \phi \sin \theta$, $y = r \sin \phi \sin \theta$ and $z = r \cos \theta$, where $r > 0$, $0 \leq \phi \leq 2\pi$ and $0 \leq \theta \leq \pi$, and factorizing the wave function by $\psi(\mathbf{r}) = R(r)Y(\theta, \phi)$. As usual, we obtain an angular differential equation

$$\left[\frac{1}{\sin \theta} \frac{\partial}{\partial \theta} \left(\sin \theta \frac{\partial}{\partial \theta} \right) + \frac{1}{\sin^2 \theta} \frac{\partial^2}{\partial \phi^2} \right] Y(\theta, \phi) = -\ell(\ell + 1) Y(\theta, \phi),$$

where

$$Y_\ell^m(\theta, \phi) = \vartheta_m \sqrt{\frac{2\ell+1}{4\pi} \frac{(\ell-|m|)!}{(\ell+|m|)!}} e^{im\phi} P_\ell^m(\cos\theta) \quad \text{and} \quad \vartheta_m \equiv \begin{cases} (-1)^m & m \geq 0 \\ 1 & m < 0 \end{cases}, \quad (4)$$

Here $\ell \in \mathbb{Z}_+$ and $m \in \mathbb{Z}$ ($|m| \leq \ell$) are respectively the angular and magnetic quantum numbers (note the calligraphic m instead of the mathtype m of the mass), and $P_\ell^m(\omega)$ are the Legendre polynomials, see e.g. [26, p. 333].

The radial differential equation, on the other hand, is a generalized extended case

$$-\frac{1}{m}(rR(r))'' + \frac{m'}{m^2}(rR(r))' + (\tilde{U}_{a,b}(r) + \tilde{V}_\ell(r))rR(r) = \tilde{E}rR(r), \quad (5)$$

which we shall study in what follows. Let us signal important differences with the one-dimensional PDM case,

- (i) the kinetic-potential has a new ambiguity-term highly depending on the position

$$\tilde{U}_{a,b}(r) = -\frac{1}{m(r)} \left[\frac{a+b}{2} \left(\frac{m'(r)}{m(r)} \right)' - \left(ab + \frac{a+b}{2} \right) \left(\frac{m'(r)}{m(r)} \right)^2 + \frac{a+b}{r} \left(\frac{m'(r)}{m(r)} \right) \right]; \quad (6)$$

- (ii) the radial effective potential reads (see Fig. 1)

$$\tilde{V}_\ell(r) \equiv \tilde{V}(r) - \frac{1}{m(r)r} \frac{m'(r)}{m(r)} + \frac{\ell(\ell+1)}{m(r)r^2}, \quad (7)$$

where the usual three-dimensional orbital “ ℓ -term” is now divided by the function $m(r)$ and the “ m -term” is completely new.

In order to solve eq. (5) we carry out a point canonical transformation

$$\frac{d\xi}{dr} = m^{1/2}, \quad (8a)$$

$$rR(r) = m^{1/4}\Xi(\xi), \quad (8b)$$

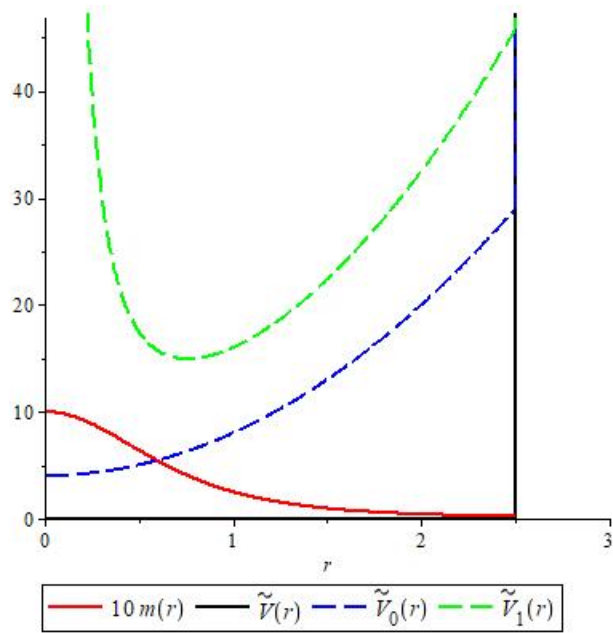
which leads to an ordinary Schrödinger equation with a highly modified effective potential,

$$-\Xi''(\xi) + V_{a,b;\ell}(\xi)\Xi(\xi) = \tilde{E}\Xi(\xi), \quad (9a)$$

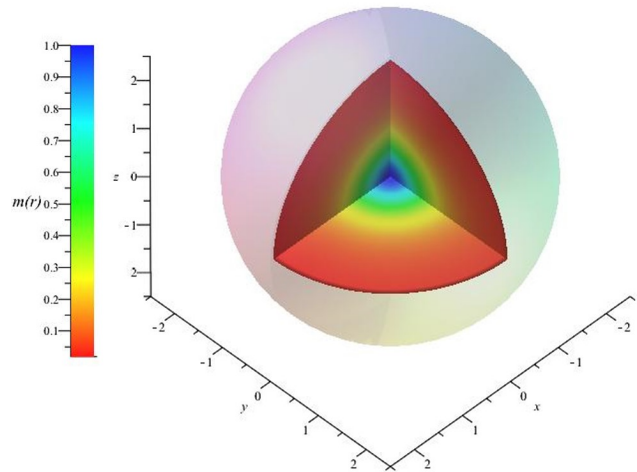
The potential term depends on the mass function and its derivatives in a nontrivial way, and on the specific ordering choice of the kinetic Hamiltonian

$$V_{a,b;\ell}(\xi) \equiv \tilde{V}(r(\xi)) + \frac{1}{m} \left[\frac{\ell(\ell+1)}{r(\xi)^2} - \frac{1}{2} \left(a+b + \frac{1}{2} \right) \left(\frac{m'}{m} \right)' + \left(ab + \frac{a+b}{2} + \frac{3}{16} \right) \left(\frac{m'}{m} \right)^2 - \frac{a+b+1}{r(\xi)} \left(\frac{m'}{m} \right) \right] \quad (9b)$$

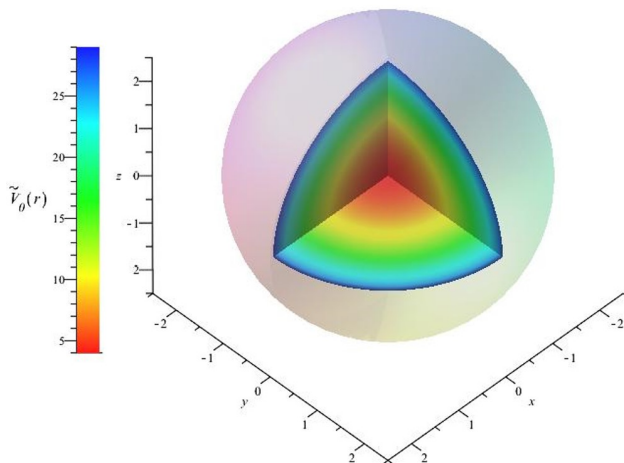
where $m = m(r(\xi))$ and the derivative $' = d/dr(\xi)$.



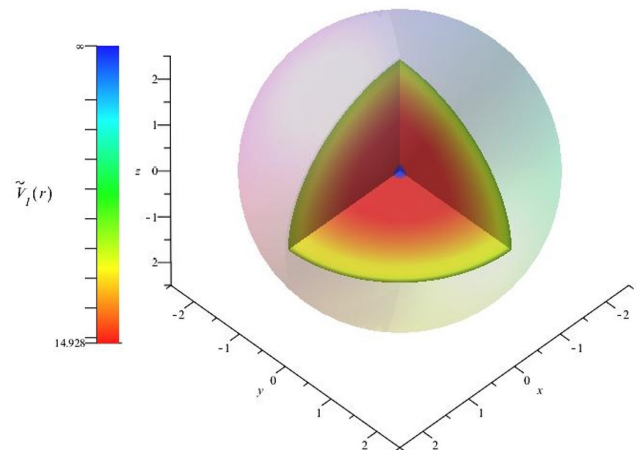
(a)



(b)



(c)



(d)

Figure 1: The position-dependent mass and some radial effective potentials for $\delta = 2.5$ in a spherical quantum dot. Figs. (b), (c) and (d) are for the three-dimensional mass (magnified for the sake of resolution), $\tilde{V}_0(\mathbf{r})$ and $\tilde{V}_1(\mathbf{r})$ respectively.

3 Mass distribution and boundary conditions

It is well known that quantum dots and few-electron transistors have definite atom-like features such as quantized energy spectra [27–29]. In order to apply our model calculations we can think of an effective carrier confined in a nanometric region. It could be for instance an electron in a semiconductor or a metal nanoparticle surrounded by an insulator or a very strong electric field, e.g. a layer of GaAs surrounded by an insulator such as AlGaAs at low temperatures [30]. The case of a perfect insulator can be modeled by a hard shell potential, and the field influence of the crystal structure on the particle by means of a position dependent mass. To specify the particle spectrum we will consider some continuous mass function confined in a region of size $\epsilon\delta$

$$m = \frac{1}{(1+r^2)^2} \quad \text{and} \quad V(\mathbf{r}) = V(r) = \begin{cases} 0 & r < \delta \\ \infty & r \geq \delta \end{cases}. \quad (10)$$

Discrete step-wise mass distributions are of course simpler to handle and rougher approaches to the problem. Continuous position-dependent masses are more subtle to represent the many particle structure and have been extensively used in the literature e.g. [13–22]. The most general treatment of continuous mass profiles, to the best of our knowledge, has been conducted in Ref. [16]. There, a full comparison among the most used continuous position-dependent masses is presented in a comprehensive calculation in one-dimensional space. In the present effort, we have also tried with a solitonic mass profile following [13–15] but we found that the analytical solution to this configuration was not possible. Thus, we decided to build the spherical quantum dot model using a steep decreasing function in order to represent a rapidly varying mass in a tiny region. This mass has another benefit which is that it has not been previously considered in three dimensions so calculations are rather novel.

The change of variables (8a) results in

$$\xi = \arctan r \Leftrightarrow r = \tan \xi, \quad (11)$$

which yields the effective potential in ξ space

$$V_{a,b;\ell}(\xi) = \ell(\ell+1) \cot^2 \xi + A_{a,b;\ell} \tan^2 \xi + B_{a,b;\ell},$$

where $A_{a,b;\ell} \equiv \ell(\ell+1) + 16ab + 10(a+b) + 6$ and $B_{a,b;\ell} \equiv 2\ell(\ell+1) + 6(a+b) + 5$. Other mass distributions can be equally considered; see e.g. [13] for a one-dimensional solitonic-like shape. In Table 1 we can see the value of these coefficients for every ordering.

In Fig. 2 we depict the effective potentials for all the relevant orderings and several orbital numbers.

Table 1: $A_{a,b;\ell}$ and $B_{a,b;\ell}$ for the relevant kinetic orderings.

Ordering	GW	ZK	LK	MM	BDD
$A_{a,b;\ell}$	$\ell(\ell+1) - 4$	$\ell(\ell+1)$	$\ell(\ell+1) + 1$	$\ell(\ell+1) + 2$	$\ell(\ell+1) + 6$
$B_{a,b;\ell}$	$2\ell(\ell+1) - 1$	$2\ell(\ell+1) - 1$	$2\ell(\ell+1) + 2$	$2\ell(\ell+1) + 2$	$2\ell(\ell+1) + 5$

In the limit of a distant spherical shell $\delta \rightarrow \infty$ (in Fig. 2, the vertical wall going towards $\xi = \pi/2$), the effective potential diverges to $-\infty$ for any $A_{a,b;\ell} < 0$ (and we must discard the fundamental states $\ell = 0$ and $\ell = 1$ for the GW ordering).

We now proceed by defining $w = \sin^2 \xi$, and $W(w)$ such that

$$\Xi(\xi) = w^{\mu_{\ell}^{\pm}} (1-w)^{\nu_{a,b;\ell}} W(w),$$

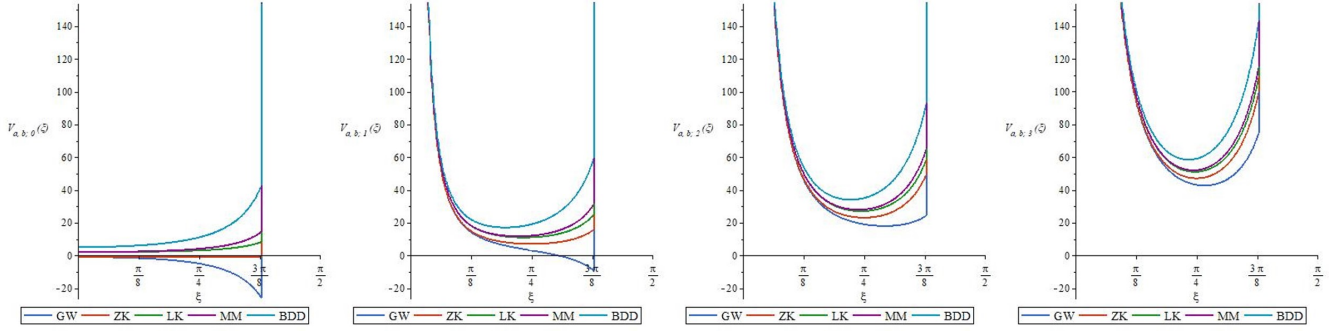


Figure 2: Graphics of $V_{a,b;\ell}(\xi)$ for $\delta = 2.5$ and some values of ℓ .

where $\mu_\ell^+ = \frac{\ell+1}{2}$, $\mu_\ell^- = -\frac{\ell}{2}$ and $v_{a,b;\ell} = \frac{1}{4} (1 - \sqrt{1 + 4A_{a,b;\ell}})$. With this, eq. (9a) results in a Gauss hypergeometric equation [31, Chap. 15],

$$\left\{ w(1-w) \frac{d^2}{dw^2} + \left[\gamma_\ell^\pm - (\alpha_{a,b;\ell}^\pm + \beta_{a,b;\ell}^\pm + 1)w \right] \frac{d}{dw} - \alpha_{a,b;\ell}^\pm \beta_{a,b;\ell}^\pm \right\} W_{a,b;\ell}^\pm(w) = 0, \quad (12)$$

where the coefficients are given by

$$\begin{aligned} \alpha_{a,b;\ell}^\pm &= \mu_\ell^\pm + v_{a,b;\ell} + \frac{1}{2} \sqrt{\Delta_{a,b}}, \\ \beta_{a,b;\ell}^\pm &= \mu_\ell^\pm + v_{a,b;\ell} - \frac{1}{2} \sqrt{\Delta_{a,b}} \quad \text{and} \\ \gamma_\ell^\pm &\equiv 2\mu_\ell^\pm + \frac{1}{2} = 1 \pm \left(\ell + \frac{1}{2} \right) \Leftrightarrow \begin{cases} \gamma_\ell^+ = \frac{3}{2} + \ell \\ \gamma_\ell^- = \frac{1}{2} - \ell \end{cases}, \end{aligned}$$

with $\Delta_{a,b} \equiv \tilde{E} + 16ab + 4(a+b) + 1$. Since $\gamma_\ell^\pm \notin \mathbb{Z}$, for each μ the two linearly independent solutions around $w = 0$ are

$$\begin{aligned} W_{a,b;\ell}^\pm(w) &= {}_2F_1 \left(\alpha_{a,b;\ell}^\pm, \beta_{a,b;\ell}^\pm; \gamma_\ell^\pm; w \right) \quad \text{and} \\ \overline{W}_{a,b;\ell}^\pm(w) &= w^{1-\gamma_\ell^\pm} {}_2F_1 \left(\alpha_{a,b;\ell}^\pm + 1 - \gamma_\ell^\pm, \beta_{a,b;\ell}^\pm + 1 - \gamma_\ell^\pm; 2 - \gamma_\ell^\pm; w \right). \end{aligned}$$

In ξ coordinates they read

$$\Xi_{a,b;\ell}^\pm(\xi) = (\sin \xi)^{2\mu_\ell^\pm} (\cos \xi)^{2v_{a,b;\ell}} {}_2F_1 \left(\alpha_{a,b;\ell}^\pm, \beta_{a,b;\ell}^\pm; \gamma_\ell^\pm; \sin^2 \xi \right). \quad (13)$$

The general solution, $\Xi_{a,b;\ell}(\xi)$, given by the linear combination of the solutions $\Xi_{a,b;\ell}^\pm(\xi)$ eq. (13), must be consistent with restriction $\lim_{r \rightarrow 0^+} rR(r) = 0$. Considering eqs. (10) and (8) it is equivalent to make $\Xi_{a,b;\ell}(\xi) \rightarrow 0$ for $\xi \rightarrow 0^+$, which excludes $\Xi_{a,b;\ell}^-(\xi)$ since it does not converge to zero at the origin. Therefore, $\Xi_{a,b;\ell}(\xi) = \mathfrak{G}_{a,b;\ell} \Xi_{a,b;\ell}^+(\xi)$, where $\mathfrak{G}_{a,b;\ell} \in \mathbb{C}$ is determined by normalization.

In ordinary radial coordinates, r , the radial solutions inside the shell can be obtained by means of eqs. (10), (8b) and (11):

$$R_{a,b;\ell}(r) = \frac{\mathfrak{G}_{a,b;\ell} r^\ell}{(1+r^2)^{\frac{\ell}{2} + v_{a,b;\ell} + 1}} {}_2F_1 \left(\alpha_{a,b;\ell}^+, \beta_{a,b;\ell}^+; \frac{3}{2} + \ell; \frac{r^2}{1+r^2} \right). \quad (14)$$

3.1 The energy spectrum

The energy spectrum $\{\tilde{E}_{a,b;\ell,n}\}_{n \in \mathbb{Z}_+}$ is obtained by imposing the boundary condition $R_{a,b;\ell}(\delta) = 0$, $\tilde{E}_{a,b;\ell,n}$ being the $(n + 1)$ -th real solution of the transcendental equation

$${}_2F_1\left(\alpha_{a,b;\ell}^+, \beta_{a,b;\ell}^+; \frac{3}{2} + \ell; \frac{\delta^2}{1 + \delta^2}\right) = 0. \quad (15)$$

The eigenstates (orbitals) are denoted by the triple (ℓ, m, n) ; note that eigenstates $(\ell, -\ell, n), \dots, (\ell, \ell, n)$ are degenerated in energy. In order to plot our results and to allow numerical comparisons we will adopt $\delta = 2.5$ while leaving free the parameters m_0 and ϵ . In Table 2 we can see the sixteen lowest quantum numbers energy bound states for each ordering.

We can obtain more information about these low lying states, for each ℓ and each ordering, by varying δ . See Fig. 3. In Fig. 4 we show the graphics of the first radial solutions.

Table 2: Energy levels for the different orderings with $\ell, n = 0, 1, 2, 3$.

		$\ell = 0$	$\ell = 1$	$\ell = 2$	$\ell = 3$
Ordering GW	$n = 0$	3.0466	14.049	33.003	60.137
	$n = 1$	23.197	41.829	67.859	101.73
	$n = 2$	57.716	83.566	116.63	157.28
	$n = 3$	106.33	139.26	179.33	226.81
Ordering ZK	$n = 0$	5.9662	17.817	37.229	64.597
	$n = 1$	26.865	45.900	72.301	106.48
	$n = 2$	61.695	87.773	121.10	162.00
	$n = 3$	110.46	143.54	183.79	231.47
Ordering LK	$n = 0$	9.6083	21.682	41.222	68.660
	$n = 1$	30.781	49.915	76.404	110.65
	$n = 2$	65.701	91.833	125.22	166.18
	$n = 3$	114.50	147.61	187.91	235.64
Ordering MM	$n = 0$	10.220	22.519	42.192	69.704
	$n = 1$	31.695	50.926	77.503	111.82
	$n = 2$	66.710	92.896	126.34	167.37
	$n = 3$	115.55	148.70	189.04	236.81
Ordering BDD	$n = 0$	15.411	28.618	48.849	76.693
	$n = 1$	38.282	57.925	84.848	119.44
	$n = 2$	73.765	100.17	133.85	175.11
	$n = 3$	122.77	156.05	196.56	244.53

3.2 Complete eigenstates

The final expressions for the complete eigenstates are obtained by taking together eqs. (4), (14) and (15), resulting, for $r < \delta$,

$$\psi_{a,b;\ell,m,n}(\mathbf{r}) = \tilde{\mathfrak{C}}_{a,b;\ell,m,n} e^{im\phi} P_\ell^m(\cos \theta) \frac{r^\ell}{(1+r^2)^{\frac{\ell}{2} + \nu_{a,b;\ell} + 1}} {}_2F_1\left(\alpha_{a,b;\ell,n}^+, \beta_{a,b;\ell,n}^+; \frac{3}{2} + \ell; \frac{r^2}{1+r^2}\right), \quad (16)$$

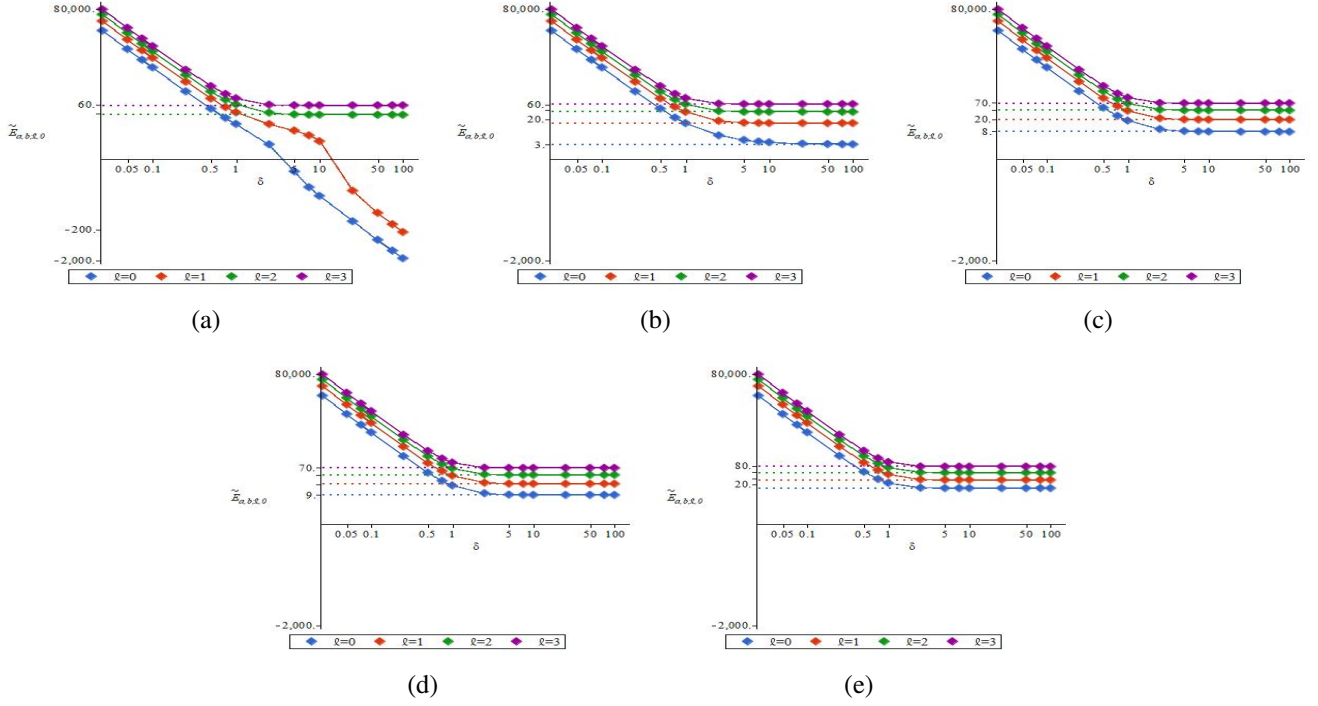


Figure 3: $\tilde{E}_{a,b;l,0}$ for the orderings (a) GW, (b) ZK, (c) LK, (d) MM and (e) BDD, with δ varying between 0.025 and 100.

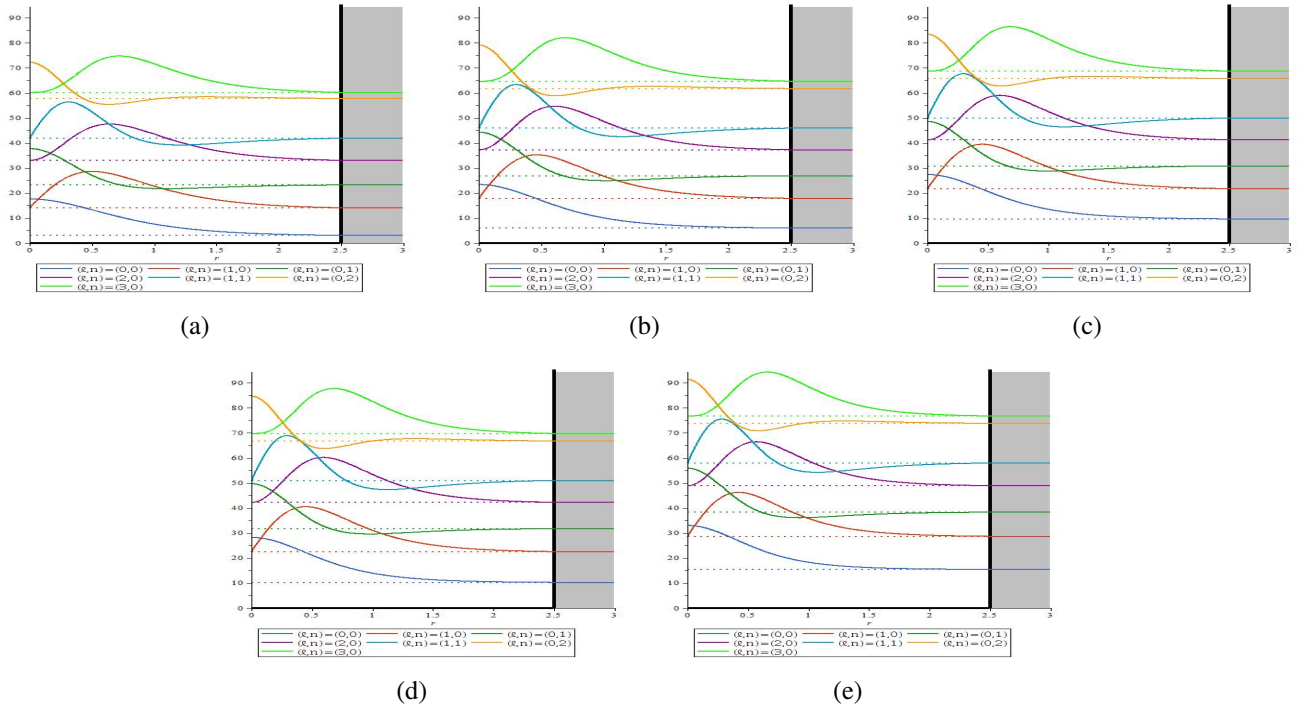


Figure 4: Radial solutions for the first seven bound-energy levels for the ordering (a) GW, (b) ZK, (c) LK, (d) MM and (e) BDD, with $\delta = 2.5$. The solid black line represents the hard wall.

and 0 otherwise. Here $\tilde{\mathfrak{C}}_{a,b;\ell,m,n} \equiv \vartheta_m \sqrt{\frac{2\ell+1}{4\pi} \frac{(\ell-|m|)!}{(\ell+|m|)!}} \mathfrak{C}_{a,b;\ell}$, with $\mathfrak{C}_{a,b;\ell} \equiv \left(\int_0^\delta |R_{a,b;\ell}(r)|^2 r^2 dr \right)^{-1/2}$. From eq. (16) we compute the probability density of the particle in three-dimensional space

$$\rho_{a,b;\ell,m,n}(\mathbf{r}) \equiv |\psi_{a,b;\ell,m,n}(\mathbf{r})|^2 = |R_{a,b;\ell,n}(r)|^2 |Y_\ell^m(\theta, \phi)|^2.$$

In Fig. 5(a) we plot the BDD ordering density $\rho_{\ell,m,n} \equiv |\psi_{0,0;\ell,m,n}|^2$ for it is the most frequently adopted in the PDM literature (the others are similar in shape). In Fig. 5(b) we show all the five orderings contour-lines for constant probability density to let clear that they are all distinct. The individual orbital graphics are organized in a growing order of energy values (horizontally, we display all the degenerated orbitals).

4 Final comments

The energy levels of a particle in a quantum dot can be computed using a three-dimensional shell model. The quantum dot absorption and emission frequencies correspond to transitions between discrete energy levels in this cell and are analogous to atomic spectra. Quantum dots are referred to as artificial atoms whereas electronic wave functions resemble the ones in real atoms [32]. In this paper we have obtained the analytical solutions for a three-dimensional position-dependent mass generalized Schrödinger equation with spherical symmetry confined in three dimensional space for five different kinetic orderings. Once boundary conditions are fixed, our exact analytical expressions depend on three quantum numbers (ℓ , m , n) and two ordering parameters a and b . We selected a smooth continuous mass profile of inverse biquadratic shape and hard shell boundary conditions which could represent effective electron carriers in a semiconductor surrounded by high vacuum or a good dielectric medium. We computed the eigenfunctions and probability densities of the first sixteen eigenstates (namely $\ell = 0, 1, 2, 3$ and $n = 0, 1, 2, 3$), for each of the five ordering levels, BDD, GW, ZK, LK and MM.

We have graphically shown the distinction among all the ordering wavefunctions together with the analytical expressions to reveal their exact differences, see eq. (15) (cf. Fig. 4). We found that the energy levels grow according to $GW \rightarrow ZK \rightarrow LK \rightarrow MM \rightarrow BDD$ (cf. Table 2). These features will eventually determine the best spectral fit to a given quantum dot experimental outcome and then the corresponding ordering choice to modeling such material. In order to further sharpen differences among orderings, we also examined the spectral behavior upon variation of δ (cf. Fig. 3). We noted

- (i) for decreasing δ the energy levels grow in an approximately exponential way;
- (ii) for growing δ the energy levels show two possible behaviors: diverge to $-\infty$ (when $A_{a,b;\ell} < 0$), or tend to a finite limit which depends on the value of the ordering parameters a , b and on ℓ (when $A_{a,b;\ell} \geq 0$); stability starts to be attained after $\delta \approx 2.5$.

Regarding the last item, when $\delta \rightarrow \infty$ the boundary condition on the radial solution $R(\delta) = 0$ can be replaced by $\Xi(\pi/2) = 0$. For $A_{a,b;\ell} < 0$ it implies a continuum spectrum with no minimal value whereas for $A_{a,b;\ell} \geq 0$ we have ${}_2F_1\left(\alpha_{a,b;\ell}^+, \beta_{a,b;\ell}^+; \gamma_\ell^+; 1\right) = 0$ which yields an analytical expression for the energy levels [31, eq. 15.1.20],

$$\tilde{E}_{a,b;\ell,n}|_{\delta \rightarrow \infty} = (2n + 2 + \ell - 2\nu_{a,b;\ell})^2 - [16ab + 4(a + b) + 1]. \quad (17)$$

In Table 3 one can verify that $\delta = 100$ serves as a good approximation to this asymptotic situation; this is tantamount to a free PDM particle in three dimensions.

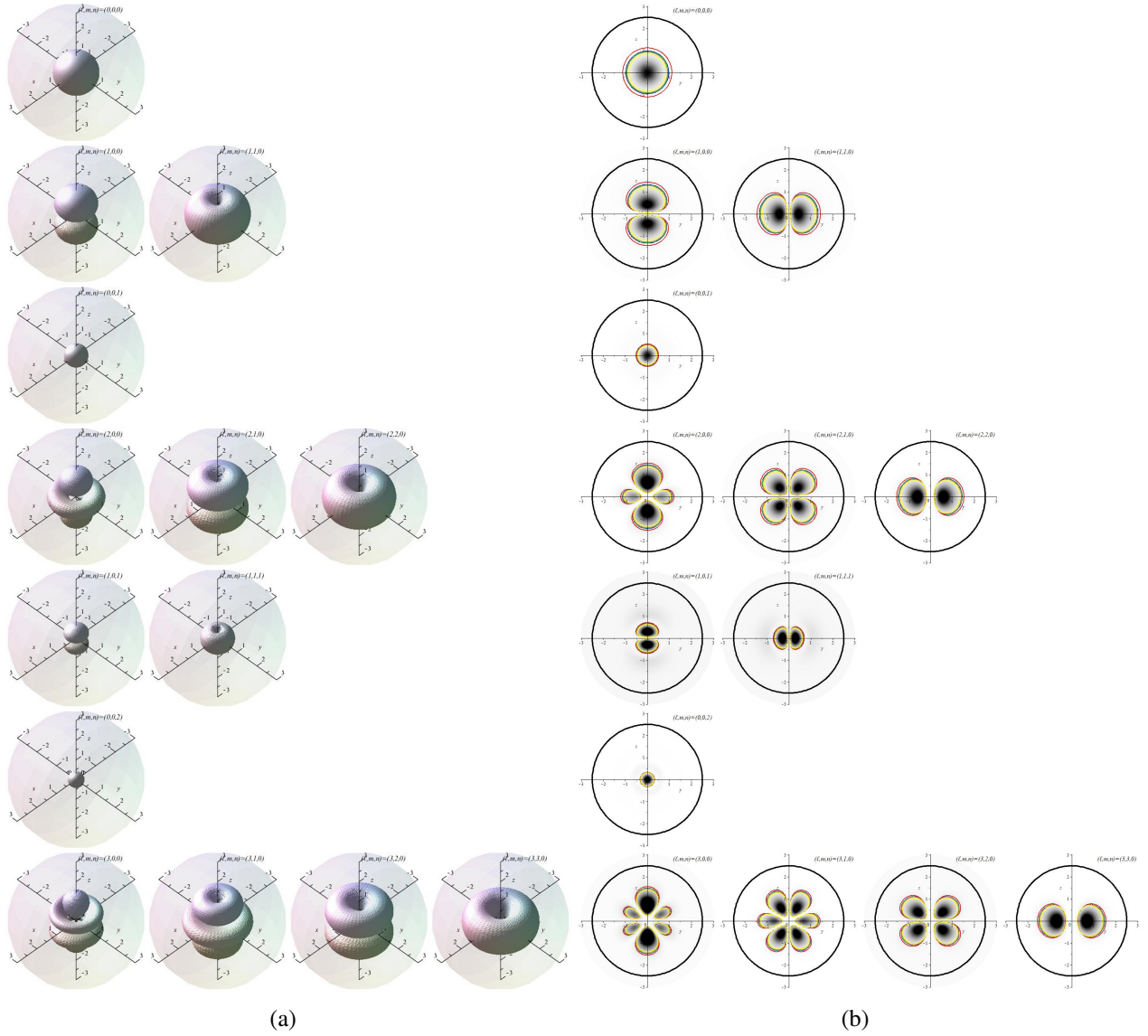


Figure 5: Three-dimensional particle probability densities $\rho_{\ell,m,n}$ for the first seven lowest energy levels (the darker shade signals the bigger probability density). (a) 3D confined particle density distributions $\rho_{\ell,m,n} = \text{cons.}$ (b) Contour lines for some particular value of $\rho_{a,b;\ell,m,n}(\mathbf{r})$ corresponding to the orderings GW (red), ZK (blue), LK (green), MM (golden) and BDD (yellow). The black circumference is for the confining shell.

Table 3: Energy levels of the lowest $n = 0$ states for large δ values from eq. (15) and eq. (17).

Ordering	$\delta = 100$				$\delta \rightarrow \infty$			
	$\ell = 0$	$\ell = 1$	$\ell = 2$	$\ell = 3$	$\ell = 0$	$\ell = 1$	$\ell = 2$	$\ell = 3$
GW	-1732.6	-240.60	28.000	57.351	$-\infty$	$-\infty$	28.	57.351
ZK	3.0514	15.000	35.000	63.000	3.	15.	35.	63.
LK	7.8547	19.514	39.348	67.260	7.8539	19.514	39.348	67.260
MM	9.0000	20.808	40.606	68.474	9.	20.808	40.606	68.474
BDD	15.000	27.861	48.000	75.948	15.	27.862	48.	75.948

The results presented in this paper are of special interest in the study of spherical quantum dots [33, p. 117]. For a typical nanostructure we can set $\epsilon \sim 10^{-9}$ m in the equations above which makes the conversion factor between \tilde{E} and E of about $\frac{0.038101}{m_0/m_e}$ eV; m_e is the free electron mass. Depending on the composition of the quantum dot one can estimate m_0/m_e from 0.01 up to order 100 or even more [34–42].

5 Acknowledgement

The authors would like to thank Conselho Nacional de Desenvolvimento Científico e Tecnológico (CNPq) for partial support.

Data Availability Statement: The authors declare that the data supporting the findings of this study are available within the paper.

Author Contribution Statement: The authors declare that they contributed equally to the research.

References

- [1] P. Harrison and A. Valavanis, *Quantum Wells, Wires and Dots – Theoretical and Computational Physics of Semiconductor Nanostructures*. New York: John Wiley & Sons, 4th ed., 2016.
- [2] L. Serra and E. Lipparini, “Spin response of unpolarized quantum dots,” *Europhys. Lett.*, vol. 40, no. 6, p. 667, 1997.
- [3] R. A. El-Nabulsi, “A generalized self-consistent approach to study position-dependent mass in semiconductors organic heterostructures and crystalline impure materials,” *Phys. E: Low Dim. Syst. Nanostruct.*, vol. 124, p. 114295, 2020.
- [4] R. Valencia-Torres, J. Avendaño, A. Bernal, and J. García-Ravelo, “Energy spectra of position-dependent masses in double heterostructures,” *Phys. Scr.*, vol. 95, p. 075207, 2020.
- [5] R. A. El-Nabulsi, “A new approach to schrodinger equation with position-dependent mass and its implications in quantum dots and semiconductors,” *J. Phys. Chem. Sol.*, vol. 140, p. 109384, 2020.
- [6] G. H. Wannier, “The structure of electronic excitation levels in insulating crystals,” *Phys. Rev.*, vol. 52, no. 3, p. 191, 1937.
- [7] J. C. Slater, “Electrons in perturbed periodic lattices,” *Phys. Rev.*, vol. 76, no. 11, p. 1592, 1949.

- [8] J. M. Luttinger and W. Kohn, “Motion of electrons and holes in perturbed periodic fields,” *Phys. Rev.*, vol. 97, no. 4, p. 869, 1955.
- [9] D. J. BenDaniel and C. B. Duke, “Space-charge effects on electron tunneling,” *Phys. Rev.*, vol. 152, no. 2, p. 683, 1966.
- [10] T. Gora and F. Williams, “Theory of electronic states and transport in graded mixed semiconductors,” *Phys. Rev.*, vol. 177, no. 3, p. 1179, 1969.
- [11] Q.-G. Zhu and H. Kroemer, “Interface connection rules for effective-mass wave functions at an abrupt heterojunction between two different semiconductors,” *Phys. Rev. B*, vol. 27, no. 6, p. 3519, 1983.
- [12] G. Bastard, *Wave mechanics applied to semiconductor heterostructures*. Les Editions de Physique, 1992.
- [13] M. S. Cunha and H. R. Christiansen, “Analytic results in the position-dependent mass Schrödinger problem,” *Commun. Theor. Phys.*, vol. 60, no. 6, p. 642, 2013.
- [14] H. R. Christiansen and M. S. Cunha, “Solutions to position-dependent mass quantum mechanics for a new class of hyperbolic potentials,” *J. Math. Phys.*, vol. 54, no. 12, p. 122108, 2013.
- [15] H. R. Christiansen and M. S. Cunha, “Energy eigenfunctions for position-dependent mass particles in a new class of molecular Hamiltonians,” *J. Math. Phys.*, vol. 55, no. 9, p. 092102, 2014.
- [16] R. M. Lima and H. R. Christiansen, “The Kinetic Hamiltonian with Position-Dependent Mass,” *Physica E: Low dimensional Systems and Nanostructures*, vol. 150, p. 115688, 2023; arXiv:2303.02507.
- [17] B. G. da Costa, I. S. Gomez, and M. Portesi, “ κ -Deformed quantum and classical mechanics for a system with position-dependent effective mass,” *J. Math. Phys.*, vol. 61, no. 8, p. 082105, 2020.
- [18] C.-L. Ho and P. Roy, “Generalized Dirac oscillators with position-dependent mass,” *Europhys. Lett.*, vol. 124, no. 6, p. 60003, 2019.
- [19] A. G. M. Schmidt and A. L. de Jesus, “Mapping between charge-monopole and position-dependent mass systems,” *J. Math. Phys.*, vol. 59, no. 10, p. 102101, 2018.
- [20] C. Chang-Ying, R. Zhong-Zhou, and J. Guo-Xing, “Exact solutions to three-dimensional Schrödinger equation with an exponentially position-dependent mass,” *Communications in Theoretical Physics*, vol. 43, no. 6, p. 1019, 2005.
- [21] H. Eleuch, P. K. Jha, and Y. V. Rostovtsev, “Analytical solution to position dependent mass for 3D-Schrödinger equation,” *Math. Sci. Lett*, vol. 1, pp. 1–6, 2012.
- [22] J. Guo-Xing, X. Yang, and R. Zhong-Zhou, “Localization of s -wave and quantum effective potential of a quasi-free particle with position-dependent mass,” *Communications in Theoretical Physics*, vol. 46, no. 5, p. 819, 2006.
- [23] O. von Roos, “Position-dependent effective masses in semiconductor theory,” *Phys. Rev. B*, vol. 27, no. 12, p. 7547, 1983.
- [24] O. Mustafa and S. H. Mazharimousavi, “Ordering ambiguity revisited via position dependent mass pseudo-momentum operators,” *Int. J. Theor. Phys.*, vol. 46, no. 7, pp. 1786–1796, 2007.

- [25] T. L. Li and K. J. Kuhn, “Band-offset ratio dependence on the effective-mass Hamiltonian based on a modified profile of the GaAs-Al_xGa_{1-x}As quantum well,” *Phys. Rev. B*, vol. 47, no. 19, p. 12760, 1993.
- [26] R. Shankar, *Principles of Quantum Mechanics*. Springer, 2nd ed., 2013.
- [27] M. Reed, J. Randall, R. Aggarwal, R. Matyi, T. Moore, and A. Wetsel, “Observation of discrete electronic states in a zero-dimensional semiconductor nanostructure,” *Phys Rev Lett*, vol. 60, pp. 535–537, 1988.
- [28] C.-L. Ho and P. Roy, “Artificial atoms,” *Phys. Today*, vol. 46, no. 1, p. 24, 1993.
- [29] R. Ashoori, “Electrons in artificial atoms,” *Nature*, vol. 379, p. 413, 1996.
- [30] M. Rakhlin, K. Belyaev, and G. e. a. Klimko, “Inas/algaas quantum dots for single-photon emission in a red spectral range,” *Sci.Rep.*, vol. 8, p. 5299, 2018.
- [31] I. A. S. Milton Abramowitz, *Handbook of Mathematical Functions with Formulas, Graphs, and Mathematical Table*. Dover Publications, 1970.
- [32] U. Banin, Y. Cao, D. Katz, and O. Millo, “Identification of atomic-like electronic states in indium arsenide nanocrystal quantum dots,” *Nature*, vol. 400, no. 6744, pp. 542–544, 1999.
- [33] D. C. Agrawal, *Introduction to nanoscience and nanomaterials*. World Scientific Publishing, 2013.
- [34] L. S. Dang, G. Neu, and R. Romestain, “Optical detection of cyclotron resonance of electron and holes in CdTe,” *Solid State Communications*, vol. 44, no. 8, pp. 1187–1190, 1982.
- [35] M. Fanciulli, T. Lei, and T. Moustakas, “Conduction-electron spin resonance in zinc-blende GaN thin films,” *Physical Review B*, vol. 48, no. 20, p. 15144, 1993.
- [36] K. Miwa and A. Fukumoto, “First-principles calculation of the structural, electronic, and vibrational properties of gallium nitride and aluminum nitride,” *Physical Review B*, vol. 48, no. 11, p. 7897, 1993.
- [37] W. Fan, M. Li, T. Chong, and J. Xia, “Electronic properties of zinc-blende GaN, AlN, and their alloys Ga_{1-x}Al_xN,” *Journal of Applied Physics*, vol. 79, no. 1, pp. 188–194, 1996.
- [38] S.-S. Li, J.-B. Xia, Z. Yuan, Z. Xu, W. Ge, X. R. Wang, Y. Wang, J. Wang, and L. L. Chang, “Effective-mass theory for InAs/GaAs strained coupled quantum dots,” *Physical review B*, vol. 54, no. 16, p. 11575, 1996.
- [39] F. Long, P. Harrison, and W. Hagston, “Empirical pseudopotential calculations of Cd_{1-x}Mn_xTe,” *Journal of applied physics*, vol. 79, no. 9, pp. 6939–6942, 1996.
- [40] R. de Paiva, R. A. Nogueira, C. de Oliveira, H. W. Alves, J. L. A. Alves, L. M. R. Scolfaro, and J. R. Leite, “First-principles calculations of the effective mass parameters of Al_xGa_{1-x}N and Zn_xCd_{1-x}Te alloys,” *Brazilian Journal of Physics*, vol. 32, pp. 405–408, 2002.
- [41] G. Margaritondo, “Semiconductor, General Properties,” in *Encyclopedia of Condensed Matter Physics* (F. Bassani, G. L. Liedl, and P. Wyder, eds.), pp. 311–321, Oxford: Elsevier, 2005.
- [42] A. Wasserman, “Effective Masses,” in *Encyclopedia of Condensed Matter Physics* (F. Bassani, G. L. Liedl, and P. Wyder, eds.), pp. 1–5, Oxford: Elsevier, 2005.